20th Australasian Fluid Mechanics Conference
Perth, Australia
5-8 December 2016

Fuel Injection and Mixing in a Mach 8 Hydrocarbon-Fuelled Scramjet

Z. J. Denman[1], V. Wheatley[1], M. K. Smart[1] and A. Veeraragavan[1]

[1]Centre for Hypersonics
The University of Queensland, Queensland 4072, Australia

Abstract

Three-dimensional, non-reacting, computational fluid dynamics simulations of an elliptical scramjet combustor with cavity flameholder are presented. The injection and mixing of gaseous methane and hydrogen fuels are examined. A one-dimensionalised inflow boundary condition, computed from full flowpath simulations of a Mach 8 shape-transitioning scramjet inlet, is used. Fuel mass flow rates were chosen to match experiments performed in the T4 Reflected Shock Tunnel, and result in equivalence ratios of approximately 0.6. The simulations show the effect that fuel injection upstream of the cavity has in a three-dimensional geometry. Further to this, hydrogen penetrates further into the core flow of the combustor compared to methane, but this results in reduced entrainment in the cavity.

Introduction

Airframe-integrated scramjet engines have become widely accepted as the most likely candidate for a scramjet-powered hypersonic vehicle [6]. High levels of integration, between the airframe and scramjet engine, places severe volume constraints on packaging requirements for the vehicle, which, in turn limits the available space for required hardware such as fuel tanks. Hydrogen has typically been the fuel of choice for scramjet engine testing due to its high specific impulse and favourable ignition characteristics, however, its low volumetric energy density (MJ/m^3) poses a significant problem for airframe-integrated scramjet engines. Figure 1 shows the benefit of using a hydrocarbon fuel from an energy density perspective. Whilst hydrogen may have twice the energy per kilogram compared to the hydrocarbon fuels, it has a far less energy per volume. This motivates the need for research on the typical energy dense fuels such as hydrocarbons.

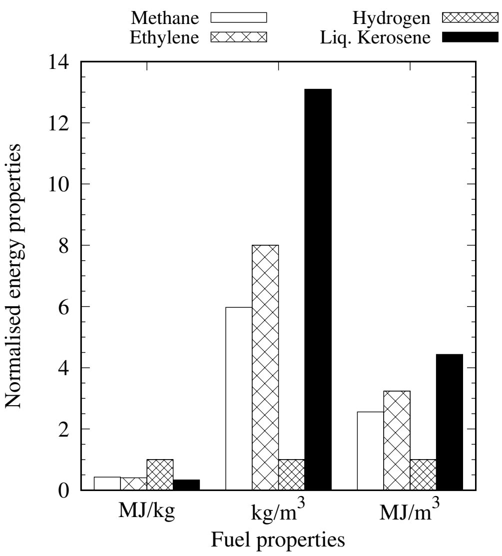

Figure 1: Fuel properties of candidate scramjet fuels [10, 13, 5]

While hydrocarbon fuels allow for increased energy storage onboard a fixed-volume scramjet-powered vehicle, their increased ignition delay times are prohibitively large for use in scramjets above Mach 7, where flow residence times are on the order of one millisecond. The ignition delay times of a number of candidate scramjet fuels are shown in Figure 2. As can be seen in Figure 2, the ignition delay time of hydrogen can be orders of magnitude less than hydrocarbon fuels at conditions likely to be encountered at the entrance to a scramjet combustor flying at Mach 8. In 1994, NASA's Chief Scientist at the Langley Research Centre noted that the ignition and flameholding of hydrocarbon fuels in scramjet engines is a first order issue [3]. Over twenty years have passed since Bushnell's statement, and research continues into methods for igniting and flameholding hydrocarbon fuels in supersonic combustors. Cavity flameholders have been proposed as a passive means by which ignition and flameholding may be achieved for hydrocarbon fuels [14, 2].

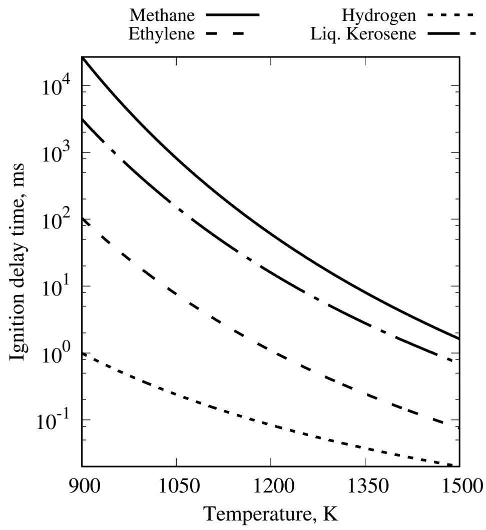

Figure 2: Ignition delay times of candidate scramjet fuels [4, 12]

Recent experiments have been performed with the HIFiRE 7 scramjet engine, which has been modified to include a cavity flameholder for the testing of hydrocarbon fuels [7, 8]. The design of this cavity is detailed in Ref. [7]. The HIFiRE 7 flowpath consists of a Rectangular-to-Elliptical shape tranitioning (REST) inlet, isolator, diverging combustor and nozzle. Figure 3 shows a photograph of the REST scramjet inlet. The inlet of the scramjet transitions from a quasi-rectangular capture area to an elliptical throat, which results in a highly complex, three-dimensional flowfield at the combustor entrance. Experiments performed in this configuration have shown that the combustion of ethylene may be achieved at a flight equivalent Mach number of 7.3 and dynamic pressure of 53.5 kPa, at an altitude of 28.7 km. Fuel was injected at the combustor entrance. The equivalence ratio of these test varied from 0.58 to 0.71.

In order to understand the injection and mixing processes that

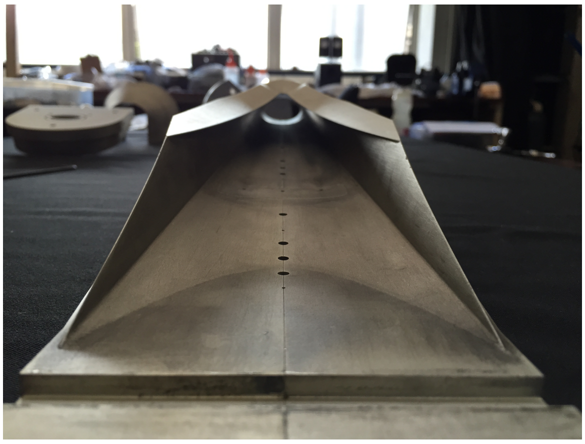

Figure 3: Photograph of shape-transitioning scramjet inlet

are occuring in the experiments with this flowpath, three-dimensional, non-reacting, simulations of HIFiRE 7 combustor, with cavity flameholder, and nozzle have been performed. The results presented in this paper document initial simulations performed with a uniform inflow into the combustor. Future simulations will use a more representative inflow taken from previous simulations of the HIFiRE 7 flowpath. Results of these future simulations will be compared to experimental data presented in Ref. [7].

Solver and Grid

The computational fluid dynamics solver used in this work is US3D, developed by Candler's group at the University of Minnesota [11]. The code solves the compressible-form of the Reynolds-averaged Navier-Stokes equations, with second order inviscid fluxes being calculated using the modified Steger-Warming method, and the viscous flux gradients computed using weighted least square fits. The Spalart-Allmaras one-equation turbulence model (in its compressive form) is used with turbulent Schmidt and Prandtl numbers of 0.7 and 0.9, respectively. The NASA Lewis database is used for determining the species properties.

The structured grid was created using GridPro v6.5 and had 21.3 million cells. The majority of the cells are located around the injectors and the cavity flameholder. The spacing of cells adjacent to the wall was set to one micrometer on all combustor surfaces, resulting in a y^+ lower than one on the majority of surfaces. The reattachment point of the shear layer on the cavity ramp and in the vicinity of the injector bow shock had higher values of y^+, but these were still less than three. A grid convergence study was not completed as the results will be compared to experimental data at a later date. However, the grid used here is comparable to other grids we have used in the past for simulations in similar scramjet engines [1, 9].

The inflow conditions for the simulation are shown in Table 1. These conditions are the one-dimensional flux-conserved conditions at the inlet throat from previous full flowpath simulations at Mach 8. The flow was assumed to be fully turbulent throughout the domain. Fuel is injected through 5 injectors (2 half injectors on the symmetry plane, and 3 full injectors). Injectors are inclined at 45° to the local flow direction and have a diameter of 1.041 millimetres. The injection conditions are shown in Table 1 and correspond to two experiments performed in the T4 Reflected Shock Tunnel; the equivalence ratio for both experiments was approximately 0.6. As this study is focussed on the injection and mixing of the fuels, chemical reactions were

	T (K)	ρ (kg/m^3)	u (m/s)	Gas
Inflow	868.2	0.2312	2067	Air
Injectors	253.3	1.1535	1211	Methane
	259.9	6.9368	413.7	Hydrogen

Table 1: Inflow conditions for simulations

suppressed.

Results

The initial results of these simulations show a high degree of three-dimensionality despite a uniform inflow condition. This is due to the elliptical shape of the combustor and cavity. This three-dimensionality may be easily seen in both temperature and equivalence ratio contours for methane (Figure 4) and hydrogen (Figure 5). The domain is symmetric along both the vertical and horizontal planes shown in Figures 4 and 5, however half of the full flowpath is still simulated as the real inflow that will be used in future simulations is not symmetric about the horizontal axis. In general, the flow structures for the two fuels simulated are similar, however, the penetration of hydrogen is slightly greater. Consequently, the fuel entrainment in the cavity for hydrogen is less compared to methane. The difference in fuel reaching the cavity is most evident when slices (b), (c), and (d) of Figure 4 and 5 are compared. In the case of Figure 5(d), practically no hydrogen is entrained in the cavity in this location.

Examination of the different slices in Figure 4, shows the effect the injector location has on the properties of the fluid in the cavity. Injectors are positioned in line with slices (a) and (e) (slice (c) is also positioned close to an injector). The flow inside the cavity downstream of the injectors is approximately 500 K cooler than between the injectors. This is due to the way the fuel plume interacts with the cavity flameholder. When the cold injected fuel reaches the cavity, it expands, following the shear layer's path. Upon reaching the shear layer's reattachment point on the aft ramp of the cavity, it deflects towards back towards the centre of the flow. The presence of the cold fuel results in a much lower temperature in the cavity downstream of the injectors.

Figure 6 shows the main way flow is entrained in the cavity. The wall pressure contours clearly show how the reattachment of the shear layer on the aft wall changes due to the injection of fuel upstream. Streamlines contoured by temperature also show how fluid is entrained in the cavity. Although only the flow around a single injector is shown, the same flow structure is present near each injector. Downstream of each injector, the flow reattaches near the beginning of the aft ramp. This results in some of the flow being entrained in the recirculation regions that form inside the cavity, between the injectors, (these locations correspond with slices (b) and (d) in Figures 4 and 5. The flow recirculates in the cavity for a brief time before being expelled. The main location at which flow is expelled from cavity is between the injectors. The bottom image of Figure 6 shows that flow between the injectors is compressed between the injector bow shocks and upon reaching the cavity moves over the cavity, merging with the flow expelled from the cavity.

Conclusions

Three-dimensional, non-reacting, numerical simulations of an elliptical combustor with cavity flameholder have been presented. Injection of methane and hydrogen has been performed and the differences in the resulting equivalence ratios in the cavity flameholder have been discussed. Despite the large difference in molecular weight, the flow features in the vicinity of

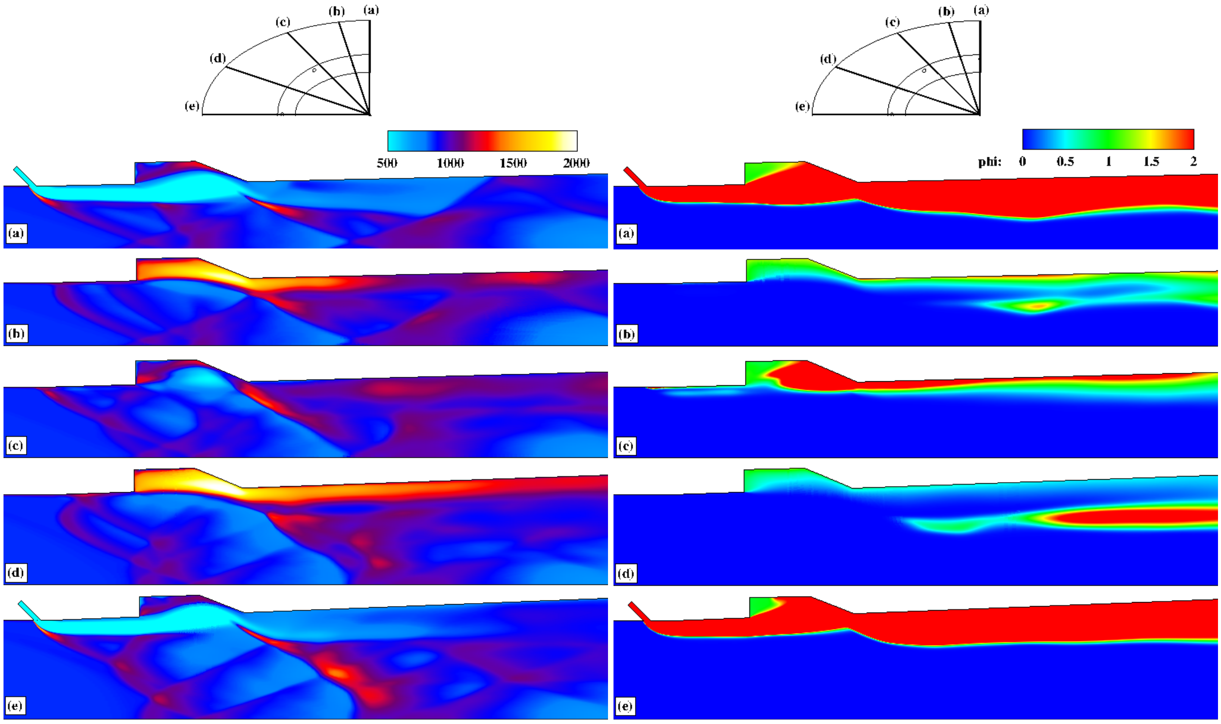

Figure 4: Temperature contours (left) and equivalence ratio (right) showing three-dimensionality of flow within cavity for methane

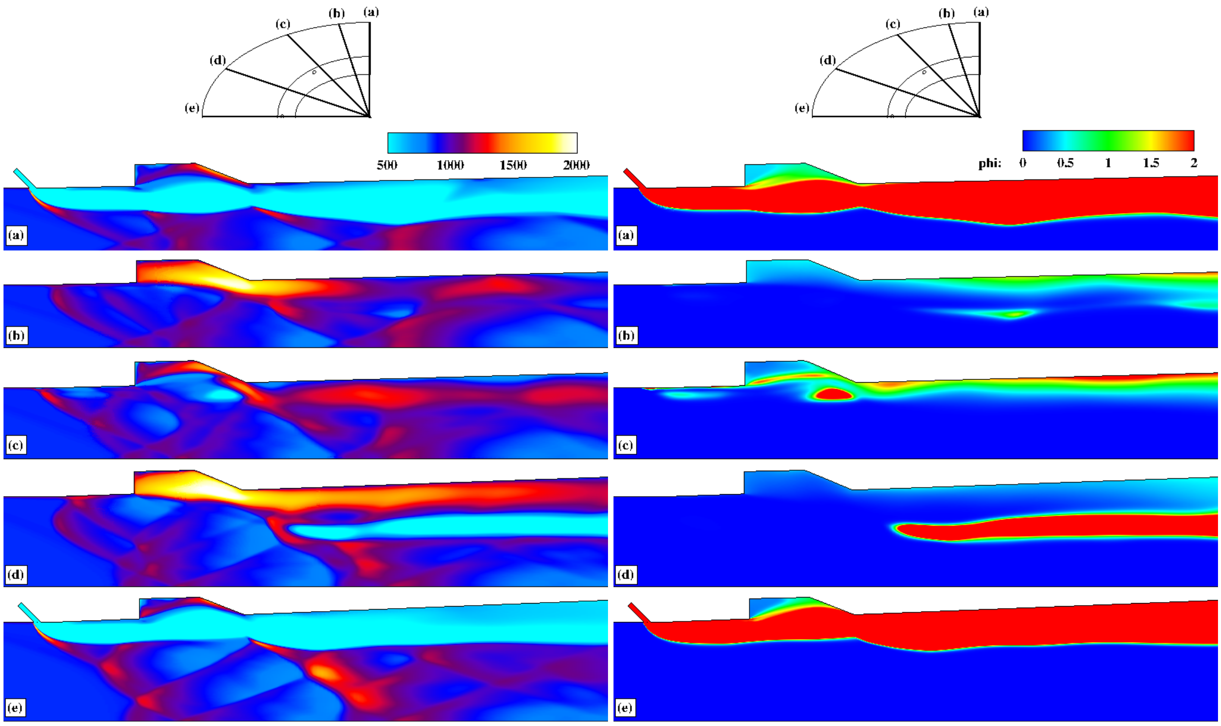

Figure 5: Temperature contours (left) and equivalence ratio (right) showing three-dimensionality of flow within cavity for hydrogen

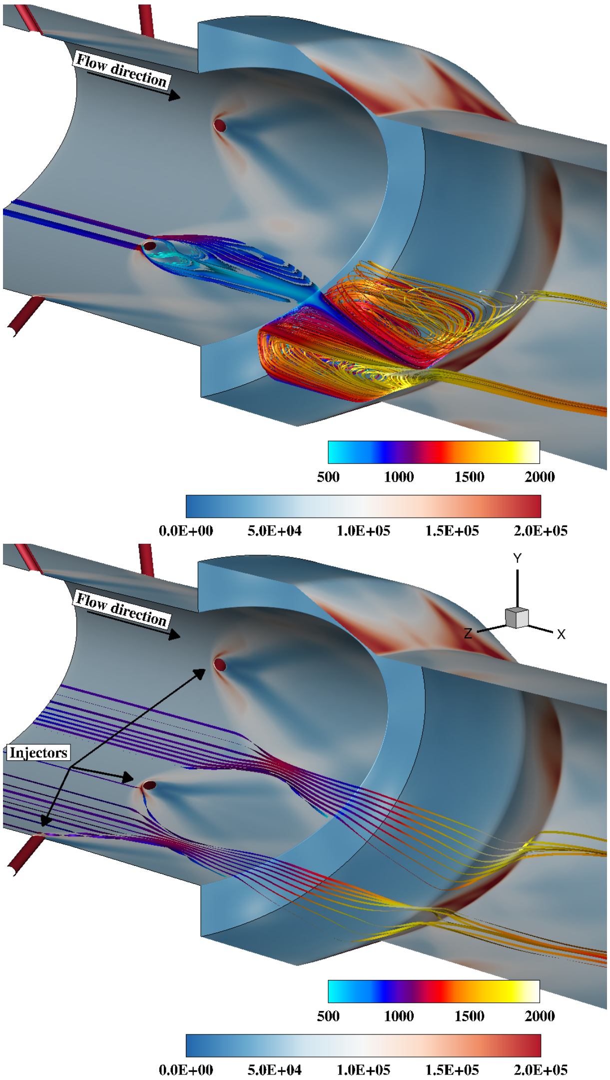

Figure 6: Wall pressure contours (Pa) and temperature streamlines (K) showing main flow in/out (top) and over (bottom) cavity

the cavity are relatively similar for both fuels. However, due to its increased penetration of the injected hydrogen into the main flow, less hydrogen is entrained within the cavity flameholder. Future simulations with this geometry will be performed using a more representative inflow at the combustor entrance, as the shape-transitioning inlet results in a highly non-uniform flow entering the combustor.

Acknowledgements

This work was supported by the AOARD under Grant No. FA2386-13-1-4060, with David Hopper as contract manager, and Chiping Li (AFOSR) as program manager. This research was undertaken with the assistance of resources provided at the NCI National Facility systems (Raijin) at the Australian National University through the National Computational Merit Allocation Scheme supported by the Australian Government. V. Wheatley was supported an Australia Research Council Discovery Early Career Researcher Award (project number DE120102942). The authors would also like to thank Will Landsberg for his assistance in performing the simulations and visualising the results.

References

[1] Barth, J. E., Wise, D. J., Wheatley, V. and Smart, M. K., Tailored fuel injection for performance enhancement in a Mach 12 scramjet engine, in *20th AIAA International Space Planes and Hypersonic Systems and Technologies Conference*, AIAA, 2015, 3614, 3614.

[2] Ben-Yakar, A. and Hanson, R. K., Cavity flame-holders for ignition and flame stabilization in scramjets: An overview, *Journal of Propulsion and Power*, **17**, 2001, 869–877.

[3] Bushnell, D. M., Mixing and combustion issues in hypersonic air-breathing propulsion, in *Combustion in high-speed flows*, Springer, 1994, 3–16.

[4] Colket, M. B. and Spadaccini, L. J., Scramjet fuels autoignition study, *Journal of propulsion and power*, **17**, 2001, 315–323.

[5] Coordinating Research Council Inc., Handbook of aviation fuel properties, Technical Report 530, Coordinating Research Council Inc., Atlanta, Georgia, 1983.

[6] Curran, E. T., Scramjet engines: the first forty years, *Journal of Propulsion and Power*, **17**, 2001, 1138–1148.

[7] Denman, Z. J., Chan, W. Y., Brieschenk, S., Veeraragavan, A., Wheatley, V. and Smart, M. K., Ignition experiments of hydrocarbons in a Mach 8 shape-transitioning scramjet engine, *Journal of Propulsion and Power*, **00**, 2016, 1–10.

[8] Denman, Z. J., Wheatley, V., Smart, M. K. and Veeraragavan, A., Supersonic combustion of hydrocarbons in a shape-transitioning hypersonic engine, *Proceedings of the Combustion Institute*, **00**, 2016, 1–9.

[9] Landsberg, W. O., Wheatley, V. and Veeraragavan, A., Characteristics of cascaded fuel injectors within an accelerating scramjet combustor, *AIAA Journal*, 1–9.

[10] Lewis, M. J., Significance of fuel selection for hypersonic vehicle range, *Journal of Propulsion and Power*, **17**, 2001, 1214–1221.

[11] Nompelis, I., Drayna, T. W. and Candler, G. V., Development of a hybrid unstructured implicit solver for the simulation of reacting flows over complex geometries, *AIAA Paper*, **2227**.

[12] Puri, P., Ma, F., Choi, J.-Y. and Yang, V., Ignition characteristics of cracked jp-7 fuel, *Combustion and Flame*, **142**, 2005, 454–457.

[13] Smukala, J., Span, R. and Wagner, W., New equation of state for ethylene covering the fluid region for temperatures from the melting line to 450 k at pressures up to 300 mpa, *Journal of Physical and Chemical Reference Data*, **29**, 2000, 1053–1121.

[14] Tishkoff, J. M., Drummond, J. P., Edwards, T. and Nejad, A. S., Future direction of supersonic combustion research: Air force/nasa workshop on supersonic combustion, *AIAA paper*, **1017**, 1997, 1–40.